

Observational constraints on α -attractor inflationary models

J. G. Rodrigues,¹ S. Santos da Costa,² and J. S. Alcaniz²

¹*Departamento de Física, Universidade Federal do Rio Grande do Norte, Natal, RN, Brazil*

²*Departamento de Astronomia, Observatório Nacional, 20921-400, Rio de Janeiro, RJ, Brazil*

(Dated: November 19, 2021)

We investigate the observational viability of a class of α -attractors inflationary models in light of the most recent Cosmic Microwave Background (CMB), Large-Scale Structure (LSS), and B-mode polarization data. Initially, from a slow-roll analysis we study the behavior of this class of models, which is a continuous interpolation between the chaotic inflation for large values of α and the universal attractor, i.e., $n_s = 1 - 2/N$ and $r = \alpha 12/N^2$ for small α , where n_s is the spectral index, r the tensor-to-scalar ratio, and N is the e-fold number. We also perform a MCMC analysis exploring the space parameter for a double-well inflationary potential, namely, a Higgs-like model. We obtain a tight constraint on the cosmological and primordial parameters for the model considered, including a 1σ -limit on the α parameter, $\alpha = 7.56 \pm 5.15$.

I. INTRODUCTION

The inflationary paradigm has become a central part of modern cosmology as it provides a good description of the first instants of the evolution of our Universe [1–3]. Since its idealization, a considerable number of inflationary models were proposed and investigated in light of observational data [4]. From the current observational perspective, the most promising scenarios rely on modified gravity theories, such as the Starobinsky model $R + R^2$ [5–7], where R is the Ricci scalar, the chaotic inflation $\lambda\phi^4$ non-minimally coupled to gravity [8–10] and a class of super-conformal inflationary theories that leads to a universal attractor behaviour [11–13].

Indeed, the most recent Cosmic Microwave Background (CMB) and Large Scale Structure (LSS) data favour models which present a plateau in their inflationary potentials [14]. In special, the Starobinsky and the non-minimal models exhibit a similar potential in the regime of large fields and strong couplings [15],

$$V(\phi) = \frac{3}{4}M^2 \left(1 - e^{-\sqrt{\frac{2}{3}}\phi}\right)^2, \quad (1)$$

where the inflaton ϕ is given in Planck units, $M_P = 1$. The energy scale M is usually constrained by the observed value of the amplitude of scalar perturbations $A_S \simeq 2.1 \times 10^{-9}$ [16]. For large values of the e-fold number, $N \gg 1$, these theories lead to the same predictions for the inflationary observable,

$$n_s = 1 - \frac{2}{N}, \quad r = \frac{12}{N^2}, \quad (2)$$

where n_s is the spectral index and r the tensor-to-scalar ratio. For $N = 60$, the expressions above yields $n_s \simeq 0.97$ and $r \simeq 0.003$, showing a remarkable agreement with present CMB observations [16].

Given their ability to describe the observed data, these inflationary scenarios and their phenomenological implications have been extensively studied [17–22]. In particular, non-minimal inflation with the Higgs field playing the role of inflaton have received a fair amount of attention, as it can potentially connect inflationary dynamics

with the low-energy phenomenology of the model. Scenarios in which extensions of the standard model drive the inflationary dynamics have also been considered in the literature [23–26].

More recently, a class of inflationary models introduced by Kalosh, Linde and Roest has received some attention given its generalist aspect [13, 27–33]. Based on the context of supergravity, the so called cosmological α -attractors stand out for achieving a slow-roll phase, even for inflationary potentials of arbitrary format $V(\phi)$ [30]. Specifically, an inflationary plateau arise in the theory due to the presence of a non-canonical kinetic term for the inflaton ϕ . Such kinetic energy features a pole at $\phi^2 = 6\alpha$, which prevents any trajectory in field space to travel beyond this limit. On the other hand, a canonical form for the Lagrangian can be achieved after a field redefinition. In the canonical field space the poles are displaced to infinity, “stretching” the scalar potential in the large field regime. Similarly to the Starobinsky inflation, such plateau at high energies seems to align the model predictions with the observational data.

Despite of all the promising characteristics of the α -attractors class of models, only the usual slow-roll investigation of this scenario has been addressed in the literature. In this sense, we aim to deepen the analysis of these models, investigating its observational viability in light of the most recent CMB, LSS and B-mode polarization data [34–39]. To this end, we use the double-well function as non-canonical potential $V(\phi)$. Such a choice finds its motivation in fundamental particle physics, where this potential can be employed in the spontaneous symmetry breaking mechanism [40–42].

This work is organized as follows. Section (II) reviews the basics of α -attractors, discussing the field redefinition to obtain the canonical inflationary Lagrangian. Section (III) shows the slow-roll analysis for the double-well potential. In Section (IV) we present the observational data sets used in our statistical analysis and the main results obtained. Finally, the main conclusions of the paper are summarized in Section (V).

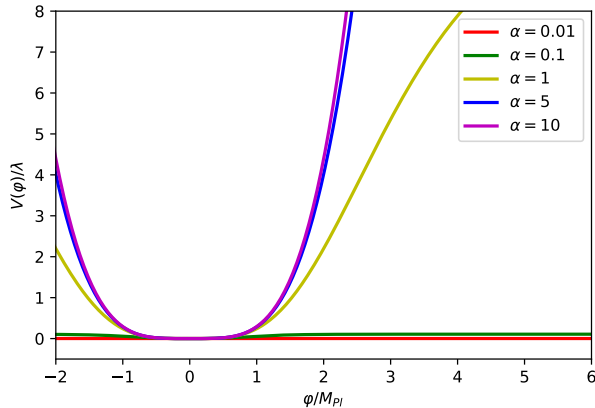


Figure 1: The Higgs-like primordial potential as a function of the canonical field φ for different values of α .

II. THE MODEL

The Lagrangian for the α -attractor class of models arise in the context of supergravity theories for specific forms of the Kähler potential,

$$\mathcal{L} = \sqrt{-g} \left[\frac{1}{2} R - \frac{1}{(1 - \phi^2/6\alpha)^2} \frac{(\partial\phi)^2}{2} - V(\phi) \right], \quad (3)$$

where ϕ is the inflaton field and α the free parameter of the theory, related to the curvature of the Kähler manifold [13]. The main characteristics of these models manifests due to the presence of a non-canonical kinetic term for the inflaton. It exhibits a pole at $\phi^2 = 6\alpha$, preventing any incursion in field space to transpose this limit. On the other hand, a canonical kinetic term can be recovered through the field redefinition,

$$\phi = \sqrt{6\alpha} \tanh \frac{\varphi}{\sqrt{6\alpha}}, \quad (4)$$

according to which the inflationary Lagrangian assumes the form,

$$\mathcal{L} = \sqrt{-g} \left[\frac{1}{2} R - \frac{(\partial\varphi)^2}{2} - V\left(\tanh \frac{\varphi}{\sqrt{6\alpha}}\right) \right]. \quad (5)$$

While the field ϕ is limited by the poles $\phi = \pm\sqrt{6\alpha}$, the canonical inflaton φ is free to assume any value in field space. As result, the scalar potential $V(\tanh \frac{\varphi}{\sqrt{6\alpha}})$ acquire a plateau in the limit of large fields, $\varphi \rightarrow \pm\infty$. Such configuration is propitious to perform large field inflation, leading to the following predictions for the inflationary observable,

$$n_S = 1 - \frac{2}{N}, \quad \text{and} \quad r = \alpha \frac{12}{N^2}, \quad (6)$$

for large N and small α .

Similarly to the Starobinsky model, the α -attractors theoretical predictions are aligned with the experiments,

at least for the slow-roll analysis. Indeed, the predictions of both scenarios coincide at leading order for $\alpha = 1$. This predictive pattern is not a coincidence, as the inflationary potential in both cases is similar at the limit of large field. Particularly, in the vicinity of $\phi = \sqrt{6\alpha}$, or equivalently $\varphi \rightarrow \infty$, the scalar potential for the canonical field can be written in the asymptotic form

$$V(\varphi) \simeq V_0 - 2\sqrt{6\alpha}V_0' \exp\left(-\sqrt{\frac{2}{3\alpha}}\varphi\right). \quad (7)$$

The expression above is reduced to the Starobinsky potential (1) for $\alpha = 1$ at leading order, except for an unobservable phase shift in φ . In this sense, one might identify the Starobinsky potential as one of the solutions of the α -attractor class, reinforcing the general aspect of these inflationary models.

Despite the general aspect of the α -attractor models at small values of α , it is fundamental to consider a specific choice of inflationary potential in order to correctly account for the predictions of the model for a broad range of α . Therefore, the slow-roll and statistical analysis of this work will focus on the double-well inflationary potential,

$$V(\phi) = \frac{\lambda}{4}(\phi^2 - v^2)^2, \quad (8)$$

where ϕ is a real inflaton and v its vacuum expectation value.

This choice of primordial potential is strongly motivated in the scope of particle physics, where it can be applied in the dynamical symmetry breaking mechanism [40–42]. In particular, the scalar sector of the standard model of fundamental particles is composed of such potential, with the scalar field behaving like a doublet under the $SU(2)_L$ standard symmetry, namely the Higgs doublet [43, 44].

As inflation takes place in the large field regime, $\phi \simeq \sqrt{6\alpha}$, it is plausible to assume that the inflationary energy scale is much bigger than the vacuum expectation value of the theory, $\phi \gg v$. Therefore, the quartic power of the non-canonical field dominates the primordial potential during inflation. After the field redefinition (4), it assumes the form,

$$V(\varphi) = 9\alpha^2\lambda \left(\tanh \frac{\varphi}{\sqrt{6\alpha}} \right)^4, \quad (9)$$

hereafter Higgs-like model.

Figure (1) shows the primordial potential, as a function of the canonical field φ , for different values of α . A flat regime is obtained for $\varphi \gg \sqrt{6\alpha}$. Such behaviour deviates the model predictions from the usual chaotic scenario. In particular, the “flattening” of the potential seems to be more efficient for lower values of α , while the canonical chaotic inflation φ^4 is recovered in the limit $\alpha \rightarrow \infty$.

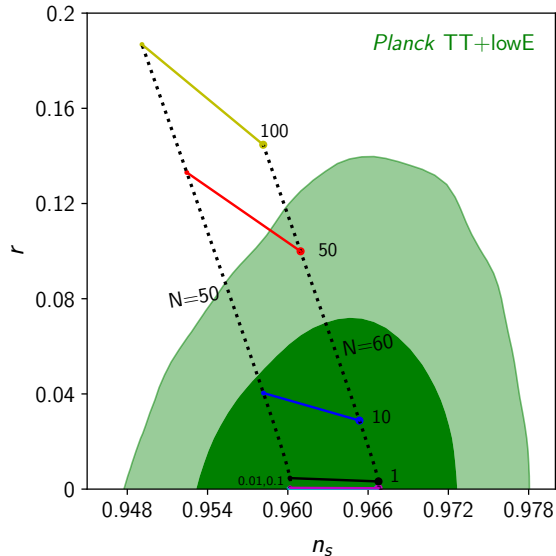


Figure 2: The $n_s - r$ plane for the Higgs-like potential (9), considering different values of the parameter α and two values for the number of e-folds, $N = 50$ and $N = 60$. The contours are the 68% and 95% confidence level regions obtained from Planck (2018) CMB data using the pivot scale $k_* = 0.05\text{Mpc}^{-1}$.

III. SLOW-ROLL ANALYSIS

Inflation and its observables are described in terms of the slow-roll parameters, ϵ and η . These parameters can be computed from the inflationary potential by

$$\epsilon = \frac{M_P^2}{2} \left(\frac{V'}{V} \right)^2, \quad \eta = M_P^2 \frac{V''}{V}, \quad (10)$$

where $'$ indicates derivative with respect to φ . The beginning of inflation occurs when $\epsilon, \eta \ll 1$ and comes to an end for $\epsilon, \eta \simeq 1$. In the slow-roll regime, the spectral index and the tensor-to-scalar ratio have the form:

$$n_s = 1 - 6\epsilon + 2\eta \quad \text{and} \quad r = 16\epsilon. \quad (11)$$

Another important observable is the amplitude of scalar perturbations, which is related with the Primordial Power Spectrum (PPS) of curvature perturbations produced during inflation:

$$A_s = P_R = \frac{V}{24M_P^4 \pi^2 \epsilon} \Big|_{k=k_*}. \quad (12)$$

By definition, these quantities are computed for the field strength φ_* , corresponding to the energy regime at which the pivot scale, k_* , crossed the Hubble horizon. The value of A_s is set by the Planck Collaboration to about 2.0933×10^{-9} for the pivot choice $k_* = 0.05\text{Mpc}^{-1}$ [16].

The field strength at horizon crossing, φ_* , can be related to the amount of expansion the universe experienced, since the horizon crossing moment up to the end of inflation. This quantity is called number of e-folds and it is defined as,

$$N_* = \frac{1}{M_P^2} \int_{\varphi_e}^{\varphi_*} \frac{V}{V'} d\varphi. \quad (13)$$

At the end of inflation the scalar potential behaves as a φ^4 function and the universe expands as radiation dominated throughout reheating [45, 46]. This case is particularly interesting because it presents a reduced uncertainty in the estimation of the e-fold number, which can be evaluated at around $N = 60$ [47].

Once the number of e-folds is set, the expression in (13) can be solved for the field strength at horizon crossing, φ_* . The resulting scale of energy is then employed to compute the model predictions for the inflationary observables. Such procedure is not possible analytically, requiring the use of numerical methods. In particular, we set the number of e-folds in the range $50 \leq N \leq 60$, in order to compare the model predictions with the Planck data.

Figure (2) shows the behavior of the spectral index and the tensor-to-scalar ratio for the model (9), considering different values of the parameter α and the number of e-folds ranging from $N = 50$ to $N = 60$. The results obtained here are in agreement with the ones presented in [13], for the family of α -attractors models of type ϕ^n . In particular, a continuous interpolation between the chaotic inflation at large α and the universal attractor (6) at small α can be noticed from that figure. For $N = 55$, the convergence at 68% (C.L.) between the model predictions and Planck data occurs for $\alpha \lesssim 28$.

The same procedure can be employed to express the amplitude λ in terms of α through the inversion of (12). In particular, we set $N = 55$ to obtain the green line in figure (3). Note that λ decreases with α up to the chaotic φ^4 value ($\lambda \simeq 10^{-13}$) in the limit $\alpha \rightarrow \infty$. Although an expression of $\lambda(\alpha)$ can not be obtained analytically, one could fit the numerical points to an analytical curve. In particular, we adjust the numerical results to the logarithmic power of α up to fifteenth order,

$$\begin{aligned}
\lambda(\alpha) \simeq & 1.36 \times 10^{-11} - 1.35 \times 10^{-11} \ln(\alpha) + 6.80 \times 10^{-12} \ln(\alpha)^2 - 2.28 \times 10^{-12} \ln(\alpha)^3 \\
& + 5.70 \times 10^{-13} \ln(\alpha)^4 - 1.14 \times 10^{-13} \ln(\alpha)^5 + 1.90 \times 10^{-14} \ln(\alpha)^6 - 2.72 \times 10^{-15} \ln(\alpha)^7 \\
& + 3.40 \times 10^{-16} \ln(\alpha)^8 - 3.78 \times 10^{-17} \ln(\alpha)^9 + 3.80 \times 10^{-18} \ln(\alpha)^{10} - 3.40 \times 10^{-19} \ln(\alpha)^{11} \\
& + 2.72 \times 10^{-20} \ln(\alpha)^{12} - 2.35 \times 10^{-21} \ln(\alpha)^{13} + 2.06 \times 10^{-22} \ln(\alpha)^{14} - 9.79 \times 10^{-24} \ln(\alpha)^{15}. \quad (14)
\end{aligned}$$

The adjusted curve is represented by the dashed line in figure (3). This expression for $\lambda(\alpha)$ will be particularly important in the investigation of observational viability of the model and parameter estimation to be performed in the next section.

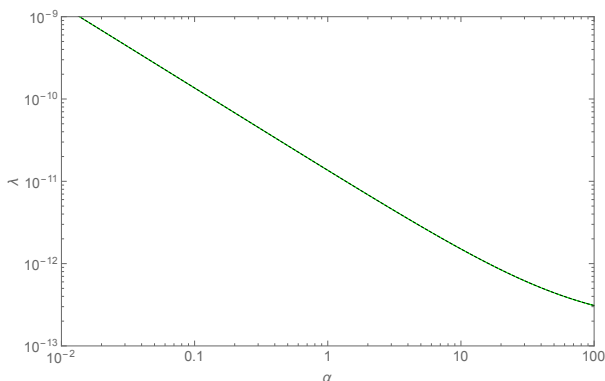


Figure 3: λ vs α computed for $N = 55$. The green line interpolates the numerical points while the dashed line shows the adjustment of the analytical curve.

IV. OBSERVATIONAL ANALYSIS AND RESULTS

In order to calculate the theoretical and observational predictions of this class of inflationary models, we modify the latest version of the Code for Anisotropies in the Microwave Background (CAMB) [48] following the lines of the MODECODE [49], adapted to our primordial potential choice (including the parameter α). On the other hand, to calculate the spectrum of CMB temperature fluctuations from the PPS, we need to solve the equations of the inflationary dynamics, i.e. the Friedmann and Klein-Gordon equations. Additionally, we also need to find the Fourier components associated with curvature perturbations produced by the fluctuations of the scalar field φ , which can be determined numerically using the MODECODE. This code solves the Mukhanov-Sasaki equations [50]

$$u_k'' + \left(k^2 - \frac{z''}{z} \right) u_k = 0, \quad (15)$$

where $u \equiv -z\mathcal{R}$ and $z \equiv a\dot{\varphi}/H$. These in turn are used to determine $\mathcal{P}_{\mathcal{R}}(k)$, that is related with u_k and z via:

$$\mathcal{P}_{\mathcal{R}}(k) = \frac{k^3}{2\pi^2} \left| \frac{u_k}{z} \right|^2. \quad (16)$$

Thus, the method consists in selecting the form of the potential $V(\varphi)$, solve the dynamics equations to obtain H and φ , and then the PPS is obtained using the solutions of the Mukhanov-Sasaki equations. As discussed before, we can use Eq. (12), given the potential $V(\varphi)$ (9), and invert it in order to determine the potential amplitude λ . Also, we have to consider the value of the field φ_* , i.e. when crossing the Hubble horizon, which can be obtained with the help of Eq. (13), using $N = 55$. This estimate was performed numerically, such that we obtained a polynomial fit of fifteenth order for $\lambda(\alpha)$, which is shown in Eq. (14).

The theoretical predictions for the Higgs-like potential (9) are shown in Fig. (4). Notice that the effect in the temperature power spectrum is a slight variation in its amplitude, which oscillates for values of the parameter α . Despite the $n_s - r$ plan shows that the value of $\alpha = 100$ is out of the 2σ region allowed by the data (for both $N = 50$ and $N = 60$), the theoretical predictions are close to the standard Λ CDM model. Therefore, we consider as an appropriate range for our analysis the flat prior of $0.01 < \alpha < 100$.

To explore the cosmological parameter space of the Higgs-like model and investigate the impact of the parameter α , we perform a Markov Chain Monte Carlo (MCMC) analysis, using the most recent version of COSMOMC code [51]. We also vary the usual cosmological parameters, namely, the baryon and the cold dark matter density, the ratio between the sound horizon and the angular diameter distance at decoupling, and the optical depth: $\{\Omega_b h^2, \Omega_c h^2, \theta, \tau\}$. We consider purely adiabatic initial conditions, fix the sum of neutrino masses to 0.06 eV and the universe curvature to zero, and also vary the nuisance foregrounds parameters [52]. The priors we considered on the cosmological parameters are shown in Table (I).

In order to compare the theoretical predictions of the model with the observational data, we use the CMB data from the latest release of Planck Collaboration (2018) [34]. We consider high multipoles Planck temperature data from the 100-, 143-, and 217-GHz half-mission T maps, and the low multipoles data by the joint TT, EE, BB and TE likelihood, where EE and BB are the E-

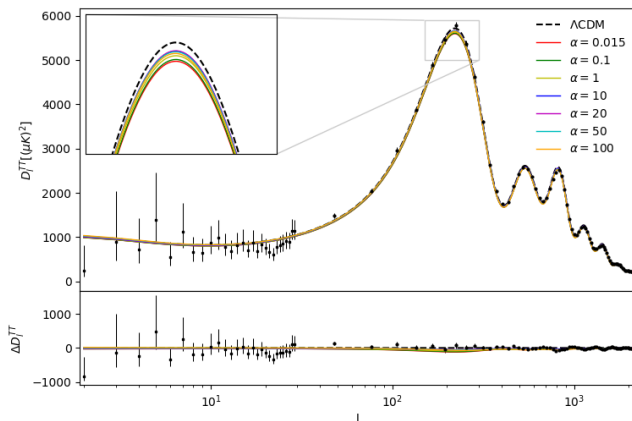


Figure 4: The theoretical predictions for the angular power spectrum considering different values of α .

Table I: Priors on the cosmological parameters considered in the analysis.

Parameter	Prior Ranges
$\Omega_b h^2$	[0.005 : 0.1]
$\Omega_c h^2$	0.001 : 0.99]
θ	[0.5 : 10.0]
τ	[0.01 : 0.8]
α	[0.01 : 100]

and B-mode CMB polarization power spectrum and TE is the cross-correlation temperature-polarization (hereafter “PLA18”). In addition, we consider an extended dataset combining the CMB data with Baryon Acoustic Oscillations (BAO) coming from the 6dF Galaxy Survey (6dFGS) [35], Sloan Digital Sky Survey (SDSS) DR7 Main Galaxy Sample galaxies [36], BOSSgalaxy samples, LOWZ and CMASS [37], and the tensor amplitude of B-mode polarization from the Keck Array and BICEP2 Collaborations [38, 39], using the BICEP2/Keck field, from 95, 150, and 220 GHz maps (hereafter “BKP15”).

The observational constraints obtained for the Higgs-like potential, using the Planck 2018 likelihood jointly with BAO and Bicep/Keck 2015 data, are summarized in Table (II) and in Figure (5). Table (II) shows the constraints on the cosmological and inflationary parameters for Higgs-like model. Note that both primary and derived cosmological parameters of Higgs-like model are in good agreement with Λ CDM within 1σ level [16]. From this analysis, we find $\alpha = 7.56 \pm 5.15$ at 68% (C.L.), a limit that is considerably more stringent than the slow-roll result $\alpha \lesssim 28$. As far as we are concerned this is the first statistical analysis constraining α -attractor inflationary models using observational data.

Figure (5) shows the confidence intervals at 68% and 95% and the posterior probability distribution for the main cosmological parameters of the Higgs-like model.

Table II: 68% confidence limits for the cosmological parameters for Higgs-like model using PLA18+BAO+BK15 data. The table is divided into two sections: the upper section shows the primary parameters, while in the lower part shows the derived ones.

Parameter	Higgs-like	
	mean	best fit
Primary		
$\Omega_b h^2$	0.02212 ± 0.018	0.02208
$\Omega_c h^2$	0.1199 ± 0.0009	0.1196
θ	1.04085 ± 0.00040	1.04108
τ	0.048 ± 0.003	0.048
α	7.56 ± 5.15	9.82
Derived		
H_0	67.16 ± 0.38	67.21
Ω_m	0.316 ± 0.005	0.320
Ω_Λ	0.684 ± 0.005	0.680
n_s	0.963 ± 0.001	0.9621
$r_{0.002}$	0.006 ± 0.002	0.008

The bounds obtained for the matter density and Hubble parameter are in accordance with Λ CDM model [16]. However, note that the limits on the tensor-to-scalar ratio are tighter than that obtained previously for both Λ CDM model and α -attractor models [13, 16, 53, 54]. Also, there is a positive correlation between α and r . Indeed, this fact can also be inferred from the $n_s - r$ plan shown in Fig. (2), which exhibits this behavior between α and r . Lastly, the figure (6) displays the temperature power spectrum for the best-fit values of the Higgs-like model, and shows a fit to the CMB data as good as the one provided by Λ CDM model.

V. DISCUSSION AND CONCLUSIONS

In this paper, we analyzed a class of inflationary models based on supergravity theories, namely, α -attractors. Specifically, we investigated the observational viability of the model for the double-well inflationary potential. Such choice is strongly motivated in the context of particle physics, presenting an ideal framework not only to successfully carry out inflation but also to connect the inflationary dynamics to low-energy phenomenology of fundamental particles. For this reason, the resulting model was called Higgs-like model.

For large values of α ($\mathcal{O}(10^2)$), the slow-roll analysis revealed that the model predictions are outside the region allowed by the data on the $n_s - r$ plan, as seen in Fig. (2). As α decreases, the predictions converge to the universal attractor values, Eq. (6). Such behavior is similar to the one predicted by a general family of cosmological attractors with $V(\varphi) \sim \varphi^n$ [13]. Extending the slow-roll study, we performed a MCMC analysis in order to explore the space parameter. The results found for the primary and derived cosmological parameters show an excellent match to the latest cosmological data as well as with the predictions of the Λ CDM model.

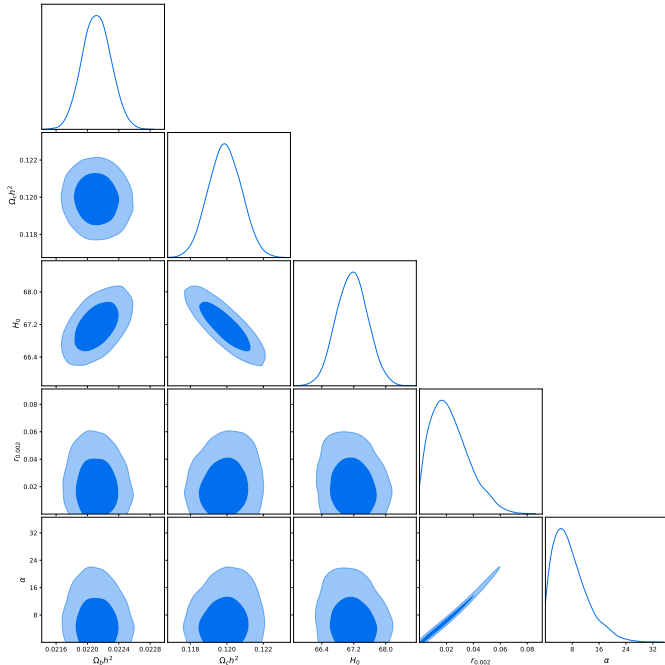


Figure 5: Two-dimensional probability distribution and one-dimensional probability distribution for the primary and derived parameters for the Higgs-like model.

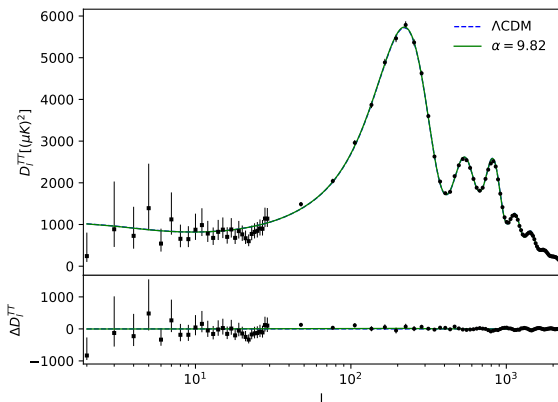


Figure 6: The best-fit angular power spectra for the Higgs-like model (green line) and Λ CDM model (blue line). The data points correspond to the latest release of Planck (2018) data and the lower panel show the residuals with respect to the reference model (Λ CDM).

We also obtained a tight constraint on the parameter α using an extended dataset including CMB, BAO, and B-mode polarization data, i.e., $\alpha = 7.56 \pm 5.15$ (68% C.L.). This result excludes the smallest values considered for α . In particular, the best-fit value for α , $\alpha = 9.82$, moves the prediction to the inflationary observable, n_S and r , farther away from the universal attractor value given by Eq. (6). This may be suggesting a substantial difference in the predictive pattern of the α -attractor models for different inflationary potentials, $V(\phi)$, in contrast to what is expected from the usual slow-roll analysis [13, 30].

It is worth mentioning that a similar analysis was also performed considering the Starobinsky potential (1) in the context of α -attractor models. The results showed no significant improvement of the constraints on the cosmological parameters with the bounds on α being not restrictive, which confirms the robustness of the Starobinsky model, as recently discussed in [55, 56].

In conclusion, we attested the observational viability of the Higgs-like attractor inflation in light of current observational data. However, further investigation about the dependence of those predictions with the choice of non-canonical potential $V(\phi)$ is needed. We shall consider this question in a forthcoming communication.

Acknowledgements

J. G. Rodrigues acknowledges Conselho Nacional de Desenvolvimento Científico e Tecnológico (CNPq) for the financial support. S. Santos da Costa thanks the financial support from the Programa de Capacitação Institucional (PCI) do Observatório Nacional/MCTI. J. Alcaniz is supported by CNPq (Grants no. 310790/2014-0 and 400471/2014-0) and Fundação de Amparo à Pesquisa do Estado do Rio de Janeiro FAPERJ (grant no. 233906). We also thank the authors of the ModeCode (M. Mortonson, H. Peiris and R. Easther) and CosmoMC (A. Lewis) codes, and the computational support of the Observatório Nacional Data Center.

[1] A. H. Guth, Phys. Rev. **D23**, 347 (1981).
[2] A. D. Linde, Phys. Lett. **108B**, 389 (1982).
[3] A. Albrecht and P. J. Steinhardt, Phys. Rev. Lett. **48**, 1220 (1982).
[4] J. Martin, C. Ringeval, and V. Vennin, Phys. Dark Univ. **5-6**, 75 (2014), 1303.3787.

[5] A. A. Starobinsky, Phys. Lett. **91B**, 99 (1980), [771(1980)].
[6] V. F. Mukhanov and G. Chibisov, JETP Letters **33**, 532 (1981).
[7] B. Whitt, Phys. Lett. B **145**, 176 (1984).
[8] D. S. Salopek, J. R. Bond, and J. M. Bardeen, Phys. Rev.

- D40**, 1753 (1989).
- [9] R. Fakir and W. G. Unruh, Phys. Rev. **D41**, 1783 (1990).
- [10] N. Makino and M. Sasaki, Prog. Theor. Phys. **86**, 103 (1991).
- [11] R. Kallosh and A. Linde, JCAP **1307**, 002 (2013), 1306.5220.
- [12] R. Kallosh, A. Linde, and D. Roest, Phys. Rev. Lett. **112**, 011303 (2014), 1310.3950.
- [13] R. Kallosh, A. Linde, and D. Roest, JHEP **11**, 198 (2013), 1311.0472.
- [14] J. Martin, C. Ringeval, R. Trotta, and V. Vennin, JCAP **03**, 039 (2014), 1312.3529.
- [15] A. Linde, M. Noorbala, and A. Westphal, Journal of Cosmology and Astroparticle Physics **2011**, 013–013 (2011).
- [16] N. Aghanim et al. (Planck) (2018), [1807.06209].
- [17] F. L. Bezrukov and M. Shaposhnikov, Phys. Lett. **B659**, 703 (2008), 0710.3755.
- [18] A. O. Barvinsky, A. Yu. Kamenshchik, and A. A. Starobinsky, JCAP **0811**, 021 (2008), 0809.2104.
- [19] J. Garcia-Bellido, D. G. Figueroa, and J. Rubio, Phys. Rev. **D79**, 063531 (2009), 0812.4624.
- [20] A. Kehagias, A. Moradinezhad Dizgah, and A. Riotto, Phys. Rev. D **89**, 043527 (2014), 1312.1155.
- [21] F. Bezrukov and M. Shaposhnikov, Phys. Lett. **B734**, 249 (2014), 1403.6078.
- [22] H. M. Lee, Phys. Rev. **D98**, 015020 (2018), 1802.06174.
- [23] R. N. Lerner and J. McDonald, Phys. Rev. **D80**, 123507 (2009), 0909.0520.
- [24] N. Okada, M. U. Rehman, and Q. Shafi, Phys. Lett. **B701**, 520 (2011), 1102.4747.
- [25] G. Ballesteros, J. Redondo, A. Ringwald, and C. Tamarit, Phys. Rev. Lett. **118**, 071802 (2017), 1608.05414.
- [26] J. G. Ferreira, C. A. de S. Pires, J. G. Rodrigues, and P. S. Rodrigues da Silva, Phys. Rev. **D96**, 103504 (2017), 1707.01049.
- [27] R. Kallosh, A. Linde, and D. Roest, JHEP **08**, 052 (2014), 1405.3646.
- [28] R. Kallosh and A. Linde, Phys. Rev. D **91**, 083528 (2015), 1502.07733.
- [29] D. Roest and M. Scalisi, Phys. Rev. D **92**, 043525 (2015), 1503.07909.
- [30] A. Linde, JCAP **1702**, 028 (2017), 1612.04505.
- [31] T. Terada, Phys. Lett. B **760**, 674 (2016), 1602.07867.
- [32] Y. Ueno and K. Yamamoto, Phys. Rev. D **93**, 083524 (2016), 1602.07427.
- [33] K. Dimopoulos and C. Owen, JCAP **06**, 027 (2017), 1703.00305.
- [34] P. Collaboration and N. A. et al., *Planck 2018 results. v. cmb power spectra and likelihoods* (2019), 1907.12875.
- [35] F. Beutler, C. Blake, M. Colless, D. H. Jones, L. Staveley-Smith, L. Campbell, Q. Parker, W. Saunders, and F. Watson, Monthly Notices of the Royal Astronomical Society **416**, 3017 (2011).
- [36] A. J. Ross, L. Samushia, C. Howlett, W. J. Percival, A. Burden, and M. Manera, Monthly Notices of the Royal Astronomical Society **449**, 835 (2015).
- [37] L. e. a. Anderson, Monthly Notices of the Royal Astronomical Society **441**, 24 (2014).
- [38] P. A. R. e. a. Ade (BICEP2/Keck and Planck Collaborations), Phys. Rev. Lett. **114**, 101301 (2015).
- [39] P. A. R. e. a. Ade (Keck Array and BICEP2 Collaborations), Phys. Rev. Lett. **116**, 031302 (2016).
- [40] J. Goldstone, Nuovo Cim. **19**, 154 (1961).
- [41] P. W. Higgs, Phys. Lett. **12**, 132 (1964).
- [42] P. W. Higgs, Phys. Rev. **145**, 1156 (1966).
- [43] S. Weinberg, Phys. Rev. Lett. **19**, 1264 (1967).
- [44] S. Weinberg, Phys. Rev. Lett. **27**, 1688 (1971).
- [45] M. S. Turner, Phys. Rev. D **28**, 1243 (1983).
- [46] V. N. Senoguz and Q. Shafi, Phys. Lett. **B668**, 6 (2008), 0806.2798.
- [47] A. R. Liddle and S. M. Leach, Phys. Rev. **D68**, 103503 (2003), astro-ph/0305263.
- [48] A. Lewis, A. Challinor, and A. Lasenby, The Astrophysical Journal **538**, 473–476 (2000).
- [49] M. J. Mortonson, H. V. Peiris, and R. Easther, Phys. Rev. **D83**, 043505 (2011), 1007.4205.
- [50] S. Weinberg, *Cosmology*, Cosmology (OUP Oxford, 2008).
- [51] A. Lewis and S. Bridle, Physical Review D **66** (2002).
- [52] N. Aghanim, M. Arnaud, M. Ashdown, J. Aumont, C. Baccigalupi, A. J. Banday, R. B. Barreiro, J. G. Bartlett, N. Bartolo, and et al., Astronomy & Astrophysics **594**, A11 (2016).
- [53] R. Kallosh and A. Linde, Physical Review D **91** (2015).
- [54] R. Kallosh, A. Linde, and D. Roest, Physical Review Letters **112** (2014).
- [55] F. Renzi, M. Shokri, and A. Melchiorri, Phys. Dark Univ. **27**, 100450 (2020), 1909.08014.
- [56] S. Santos da Costa, M. Benetti, J. Alcaniz, R. Silva, and R. Neves (2020), 2007.09211.